INTERNATIONAL JOURNAL OF OPTIMIZATION IN CIVIL ENGINEERING
Int. J. Optim. Civil Eng., 2026; 16(3):375-403

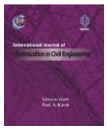

OPTIMAL DESIGN OF DUAL STEEL FRAME STEEL SHEAR WALL SYSTEMS USING A LEVY FLIGHT ENHANCED PUMA OPTIMIZATION ALGORITHM

R. Sepehri, H. Azizian[*, †], R. Sojoudizadeh, and S. Salehian
Department of Civil Engineering, Mah.C., Islamic Azad University, Mahabad, Iran

[DOI: 10.22068/ijoce.2026.16.3.671]

ABSTRACT

The dual steel system comprising moment-resisting frames integrated with steel shear walls represents an advanced seismic-resistant solution in structural engineering. This system synergistically combines the high ductility and energy dissipation capacity of steel frames with the substantial lateral stiffness and strength provided by steel shear walls. Proper design of such systems requires precise determination of the optimal location, thickness, and mechanical properties of the shear walls parameters that critically govern seismic performance, structural safety, material efficiency, and construction cost. To achieve an optimal balance between performance and economy, the problem is formulated as a constrained optimization task. This study employs the recently developed Puma Optimizer (PO) and introduces a novel enhanced variant, termed the Upgraded Puma Optimizer (U-PO). The key novelty of this work lies in the integration of Lévy flight distribution into the PO framework, replacing conventional Brownian motion to significantly strengthen the exploration–exploitation balance, global search capability, and convergence speed. This modification enables more effective handling of complex, high-dimensional structural optimization problems. The performance of the proposed U-PO is rigorously evaluated through the optimal design of three benchmark steel frames (1-, 10-, and 20-story) equipped with shear walls. The primary objective is to minimize the total structural weight while satisfying strength, serviceability, and seismic design requirements according to relevant building codes. Decision variables include frame member cross-sections as well as the location and thickness of shear walls. Comparative results against several established metaheuristic algorithms (HHO, AOA, and GWO) demonstrate the superiority of the U-PO, confirming that the incorporation of Lévy flights leads to markedly improved convergence behavior and solution quality. The U-PO consistently yields superior designs featuring notable reductions in structural weight through more efficient sizing and strategic placement of steel shear walls.

---

[*]Corresponding author: Department of Civil Engineering, Mah.C., Islamic Azad University, Mahabad, Iran
[†]E-mail address: hadi.azizian@iau.ac.ir (H. Azizian)

Keywords: Steel shear walls; Metaheuristic optimization; Puma Optimizer; Lévy flight; Structural weight minimization.

Received: 10 June 2026; Accepted: 02 August 2026

[DOI: 10.22068/ijoce.2026.16.3.671]

1. INTRODUCTION

Structural optimization is a sophisticated engineering discipline that seeks to enhance the performance, efficiency, and sustainability of structures while minimizing material consumption, cost, and environmental impact. This field integrates advanced computational techniques, including topology optimization, which determines the optimal material distribution within a prescribed design domain, and sensitivity analysis combined with numerical methods to effectively handle shape and size optimization by systematically adapting structural boundaries. Over recent decades, structural optimization has witnessed remarkable progress. Early studies primarily relied on mathematical programming and sensitivity-based approaches, laying the foundation for modern structural design frameworks [1]. Subsequent research has increasingly adopted metaheuristic algorithms, such as genetic algorithms, offering greater adaptability and robustness in solving complex, nonlinear problems [2]. The integration of high-fidelity simulation tools, uncertainty quantification, and probabilistic methods has further advanced the field, enabling more reliable and robust designs [3–5]. Moreover, emerging trends incorporating machine learning and real-time data-driven methodologies are poised to redefine the future of structural optimization [6].

Steel shear walls constitute a critical lateral load-resisting system in steel structures. These systems typically comprise thin steel plates connected to surrounding beams and columns, forming continuous vertical elements that efficiently resist in-plane shear forces. Beyond providing substantial lateral stiffness and strength, steel shear walls exhibit favorable seismic characteristics, including high initial stiffness, significant ductility, and excellent energy dissipation capacity under cyclic loading. The adjacent beams and columns act as horizontal and vertical boundary elements, respectively. Due to their superior seismic performance, steel shear walls are widely employed in both new constructions and the retrofitting of existing buildings.

Numerous experimental and numerical studies have investigated the behavior of steel plate shear walls. Astaneh-Asl et al. [7] highlighted their exceptional seismic resistance in steel structures. Alinia and Dastfan [8] examined the influence of boundary conditions on the buckling and post-buckling behavior of thin steel plate shear walls, demonstrating that flexural rigidity of boundary members has limited impact on overall performance, whereas torsional rigidity primarily affects elastic buckling strength. Jahanpour et al. [9] proposed design modifications for floor beams in semi-supported steel shear walls to improve seismic performance.

More recent experimental investigations by Rahnavard et al. [10] on composite steel-concrete shear walls under cyclic loading revealed that optimizing concrete thickness and connector spacing can significantly enhance energy dissipation and delay buckling. Paslar et al. [11] emphasized the critical role of infill plate connections in determining the strength, ductility, and overall behavior of shear wall systems. He et al. [12] employed an improved genetic algorithm (IGA) to optimize the layout and size of steel plate shear walls (SPSWs) in 5-, 10-, and 20-story steel frames, demonstrating that layout optimization can reduce the total structural weight by approximately 10–25% compared to conventional size optimization while achieving better utilization of structural elements and satisfactory seismic performance. Saedi et al. [13] employed a modified dolphin echolocation algorithm to optimize steel frames equipped with shear walls, achieving up to a 10% reduction in structural weight while satisfying seismic and design code requirements.

Gholizadeh et al. [14] proposed a modified sine-cosine algorithm in which the worst solutions were replaced with variants of the global best solution and an efficient mutation operator was incorporated, resulting in improved performance and enhanced avoidance of local optima. Kaveh and Eskandari [15] proposed an MSPA-based parameter tuning strategy that improved the efficiency of metaheuristic optimization algorithms. They also evaluated several neural network models for the analysis of double-layer barrel vaults and the prediction of maximum element stresses [16].

In recent decades, structural optimization has received considerable attention in civil engineering, with extensive contributions from Kaveh et al. [17–21] through the development of various advanced metaheuristic algorithms such as charged system search, quantum evolutionary methods, jellyfish search optimizer, and their applications in optimal design of structures. The increasing demand for efficient and economical structural designs has underscored the vital role of optimization algorithms that systematically search for optimal solutions satisfying multiple constraints while minimizing weight and improving seismic performance. Traditional mathematical programming methods often suffer from premature convergence to local optima, particularly in highly nonlinear and multimodal problems. Consequently, metaheuristic and stochastic algorithms have gained prominence for their superior global search capabilities and effectiveness in solving complex engineering optimization problems.

The present study employs advanced metaheuristic techniques to optimize the seismic design of steel frame structures integrated with steel shear wall systems. The primary objective is to determine the optimal placement and thickness of steel shear walls in multi-story buildings so as to minimize the total structural weight while satisfying all strength, serviceability, and seismic design requirements. For this purpose, the recently developed Puma Optimizer (PO) [22] is utilized. To overcome the limitations of conventional metaheuristic algorithms in complex, high-dimensional structural optimization problems, this study proposes a novel enhanced variant termed the Upgraded Puma Optimizer (U-PO). The key contribution of this work is the integration of Lévy flight distribution into the PO framework, replacing traditional Brownian motion randomization. This modification significantly improves the exploration–exploitation balance, global search capability, and convergence rate, leading to superior optimization performance compared with the standard PO and other well-established metaheuristics such as HHO, AOA, and GWO.

The effectiveness of the proposed U-PO is evaluated through the optimal design of three benchmark steel frames with 1, 10, and 20 stories. The objective function is defined as the minimization of total structural weight, with decision variables including the cross-sectional dimensions of frame members and the location and thickness of shear walls. Comparative results demonstrate the superiority of the U-PO in achieving more economical and high-performance seismic-resistant steel structures. This research advances the field of

[DOI: 10.22068/ijoce.2026.16.3.671]

metaheuristic optimization by refining newly introduced algorithms and showcasing their practical applicability in real-world structural engineering problems.

2. OPTIMIZATION PROBLEM STATEMENT

This section presents the mathematical formulation of the optimization problem for the seismic design of dual steel systems comprising moment-resisting frames and steel shear walls. The primary objective is to minimize the total structural weight while satisfying all strength, serviceability, and seismic design constraints. The optimization process employs discrete design variables, whereby each structural member (beams, columns, and shear walls) is assigned a predefined cross-sectional profile from a standard steel section database.

Let S = {S1, S2,…, Sn} represent the predefined set of discrete cross-sectional areas available for selection during the optimization process.

$$Weight\ (\boldsymbol{A}) = \sum_{i=1}^{e} \rho_i\, I_i\, A_i\,. \qquad i = 1.2.\ldots.e, \tag{1}$$

where, ρ_i stands for the steel material's density; the vector A includes the cross-sectional area of the design sections (A_i); e denotes the number of structural elements and I_i represents the structural elements' total length in the considered steel frame structure.

The design variables are treated as discrete variables to define the cross-sectional area of the chosen steel wide-flange section from a predefined list ($A \in S_f$). Additionally, other discrete variables are used to determine the position and cross-section of the steel shear walls ($W \in S_w$) as follows:

$$\boldsymbol{A} \in \boldsymbol{S_f} = \{A_1\,.A_2\,.\ldots.A_i\} \tag{2}$$

$$\boldsymbol{W} \in \boldsymbol{S_w} = \{W_1\,.W_2\,.\ldots.W_i\} \tag{3}$$

where $\boldsymbol{S_w}$is the vector of design variables representing all steel shear wall specifications ;including thickness and placement; and $\boldsymbol{S_f}$ is the vector containing the discrete wide-flange sections assigned to beams and columns. The design constraints are formulated according to the maximum allowable nodal displacements of the steel frame and the combined stresses in the structural members, as follows:

$$\delta_{min} \le \delta_j \le \delta_{max}. \qquad j = 1.2.\ldots.n, \tag{4}$$

$$\sigma_{min} \le \sigma_i \le \sigma_{max}. \qquad i = 1.2.\ldots.e, \tag{5}$$

where, σ_i represents stress in the i^{th} structural element; n represents the number nodes in the structure; δ_j stand for the nodal displacement in the j^{th} node; δ_{max} and σ_{max} represent the upper limits of the allowable stress and nodal displacement , respectively, while δ_{min} and σ_{min} denote the corresponding lower bounds. Given the presence of multiple behavioral and side

[DOI: 10.22068/ijoce.2026.16.3.671]

constraints in the optimization of dual steel frame–shear wall systems, a penalty function method is adopted to incorporate the constraints into the objective function. The constraint violation handling procedure is defined as follows:

$$f_{penalty}(\boldsymbol{A}) = (1 + \varepsilon_1 , v)^{\varepsilon_2} \times Weigth\ (\boldsymbol{A}) \tag{6}$$

$$v = \sum_{i=1}^{h} max\{0. g_i(\boldsymbol{A})\} \tag{7}$$

where, h denotes the total count of design constraints; ε_1 and ε_2 are employed to regulate the penalty imposed on the constraints; g_i (A) signifies the i^{th} design constraint; v signifies the sum of the breached design constraints.

3. PUMA OPTIMIZER (PO)

This section describes the metaheuristic algorithms adopted for the optimal design of steel shear walls integrated into steel moment-resisting frames. The principal optimization algorithm employed in this study is the Puma Optimizer (PO). Furthermore, an enhanced version of this algorithm, termed the Upgraded Puma Optimizer (U-PO), is proposed and systematically investigated. For performance evaluation, the results obtained by the PO and U-PO are compared with those of three well-established metaheuristic algorithms: the Harris Hawks Optimizer (HHO) [23], the Arithmetic Optimization Algorithm (AOA) [24], and the Grey Wolf Optimizer (GWO) [25]. These comparative analyses serve to validate the effectiveness and superiority of the proposed PO and U-PO algorithms in addressing the challenging optimization problem associated with dual steel frame–shear wall systems.

The puma (Puma concolor), also known as the cougar or mountain lion (Fig. 1), is a large felid belonging to the subfamily Felinae and native to the Americas. This highly adaptable predator occupies a broad range of habitats and exhibits a versatile diet. It is recognized as the fourth largest cat species worldwide and is noted for its exceptional agility and lean physique. Adult males typically stand 60–90 cm at the shoulder and reach a total length of approximately 2.4 meters from nose to tail tip. Primarily nocturnal, pumas may also be active during daylight hours. Their diet consists mainly of ungulates, particularly deer, which they hunt using ambush tactics. They also consume smaller prey such as rodents and insects and occasionally target domestic animals. Pumas preferentially inhabit areas with dense vegetation and rugged terrain that provide cover for stalking, although they can also be found in more open landscapes. Like most felids, they are territorial and maintain large home ranges. While capable of short bursts of speed, pumas typically rely on stealth, stalking through underbrush before launching a powerful leap to subdue prey, which is dispatched with a strong bite to the neck.

[DOI: 10.22068/ijoce.2026.16.3.671]

Figure 1: A Puma in the nature [22]

The Puma Optimizer (PO) is a novel metaheuristic algorithm inspired by the hunting behavior and territorial characteristics of pumas in their natural habitat. The algorithm translates key behavioral patterns of this predator into a mathematical framework to effectively solve complex optimization problems. Similar to other metaheuristic approaches, PO initiates the search process with a population of randomly generated candidate solutions and iteratively improves them through mechanisms that balance exploration and exploitation of the search space. In this model, the current best solution is analogous to a dominant male puma, the entire search space represents its territory, and the remaining candidate solutions correspond to female pumas. In the PO algorithm, exploration and exploitation phases occur simultaneously during the first three iterations as part of the initialization process, prior to the main phase transition. The detailed procedures implemented in this stage are presented below:

$$f1_{Explor} = PF_1 \cdot \left(\frac{Seq^1_{Cost\ Explore}}{Seq_{Time}}\right) \tag{8}$$

$$f1_{Exploit} = PF_1 \cdot \left(\frac{Seq^1_{Cost\ Exploit}}{Seq_{Time}}\right) \tag{9}$$

$$f2_{Explor} = PF_2 \cdot \left(\frac{Seq^1_{Cost\ Explore} + Seq^2_{Cost\ Explore} + Seq^3_{Cost\ Explore}}{Seq^1_{Time} + Seq^2_{Time} + Seq^3_{Time}}\right) \tag{10}$$

$$f2_{Exploit} = PF_2 \cdot \left(\frac{Seq^1_{Cost\ Exploit} + Seq^2_{Cost\ Exploit} + Seq^3_{Cost\ Exploit}}{Seq^1_{Time} + Seq^2_{Time} + Seq^3_{Time}}\right) \tag{11}$$

[DOI: 10.22068/ijoce.2026.16.3.671]

$$\mathrm{Seq}^{1}_{\mathrm{Cost\ Explore}} = \left|\mathrm{Cost}^{\ Initial}_{\ \mathrm{Best}} - \mathrm{Cost}^{\ 1}_{\ \mathrm{Explore}}\right| \tag{12}$$

$$\mathrm{Seq}^{2}_{\mathrm{Cost\ Explore}} = \left|\mathrm{Cost}^{\ 2}_{\ \mathrm{Explore}} - \mathrm{Cost}^{\ 1}_{\ \mathrm{Explore}}\right| \tag{13}$$

$$\mathrm{Seq}^{3}_{\mathrm{Cost\ Explore}} = \left|\mathrm{Cost}^{\ 3}_{\ \mathrm{Explore}} - \mathrm{Cost}^{\ 2}_{\ \mathrm{Explore}}\right| \tag{14}$$

$$\mathrm{Seq}^{1}_{\mathrm{Cost\ Exploit}} = \left|\mathrm{Cost}^{\ Initial}_{\ \mathrm{Best}} - \mathrm{Cost}^{1}_{\mathrm{Exploit}}\right| \tag{15}$$

$$\mathrm{Seq}^{2}_{\mathrm{Cost\ Exploit}} = \left|\mathrm{Cost}^{2}_{\mathrm{Exploit}} - \mathrm{Cost}^{1}_{\mathrm{Exploit}}\right| \tag{16}$$

$$\mathrm{Seq}^{3}_{\mathrm{Cost\ Exploit}} = \left|\mathrm{Cost}^{3}_{\mathrm{Exploit}} - \mathrm{Cost}^{2}_{\mathrm{Exploit}}\right| \tag{17}$$

where Seq_{Time} is a constant integer equal to 1, and PF_1 and PF_2 are fixed parameters that must be tuned prior to the optimization process. Here, f denotes the objective function value, with $\mathrm{Cost}^{\ Initial}_{\ \mathrm{Best}}$ representing the best objective value obtained during the initial solution search phase, and $\mathrm{Cost}^{\ \mathrm{i}}_{\ \mathrm{Explore}}$ identifying the best candidate solution in each phase. The transition between the exploration and exploitation phases is determined based on the collective experience of the puma population. This decision is made by identifying the endpoints of each phase according to the procedure illustrated in Fig. 2.

$$Score_{Explore} = (PF_1 \cdot f1_{Explor}) + (PF_2 \cdot f2_{Explor}) \tag{18}$$

$$Score_{Exploit} = (PF_1 \cdot f1_{Exploit}) + (PF_2 \cdot f2_{Exploit}) \tag{19}$$

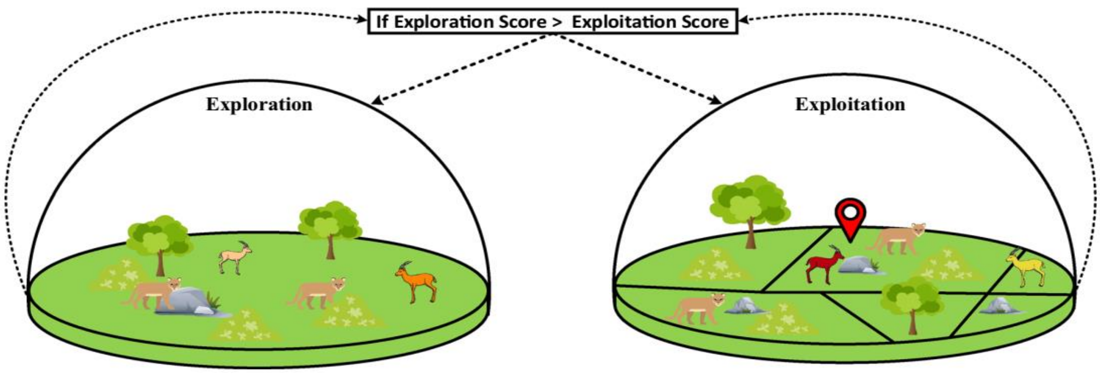

Figure 2: Exploration and Exploitation procedures in the PO

After the first three iterations, the algorithm enters the experienced phase, wherein the puma population is considered to possess sufficient knowledge for effective phase transition decisions. The search process is subsequently driven by three primary mathematical functions: a fitness evaluation function, a resonance function that emphasizes high-quality regions of the search space, and a switching mechanism that determines the appropriate transition between the exploitation and exploration phases.

[DOI: 10.22068/ijoce.2026.16.3.671]

$$f_{1\,t}^{\;exploit} = PF_1 \cdot \left|\frac{Cost_{old}^{exploit} - Cost_{new}^{exploit}}{T_t^{exploit}}\right| \tag{20}$$

$$f_{1\,t}^{\;explore} = PF_1 \cdot \left|\frac{Cost_{old}^{explore} - Cost_{new}^{explore}}{T_t^{explore}}\right| \tag{21}$$

$$f_{2\,t}^{\;exploit} = PF_2 \cdot \left|\frac{\left(Cost_{Old.1}^{exploit} - Cost_{New.1}^{exploit}\right) + \left(Cost_{Old.2}^{exploit} - Cost_{New.2}^{exploit}\right) + \left(Cost_{Old.3}^{exploit} - Cost_{New.3}^{exploit}\right)}{T_{t.1}^{exploit} + T_{t.2}^{exploit} + T_{t.3}^{exploit}}\right| \tag{22}$$

$$f_{2\,t}^{\;explore} = PF_2 \cdot \left|\frac{\left(Cost_{Old.1}^{explore} - Cost_{New.1}^{explore}\right) + \left(Cost_{Old.2}^{explore} - Cost_{New.2}^{explore}\right) + \left(Cost_{Old.3}^{explore} - Cost_{New.3}^{explore}\right)}{T_{t.1}^{explore} + T_{t.2}^{explore} + T_{t.3}^{explore}}\right| \tag{23}$$

$$f_{3\,t}^{\;exploit} = \begin{cases} if\ selected. & f_{3\,t}^{\;exploit} = 0 \\ otherwise. & f_{3\,t}^{\;exploit} + PF_3 \end{cases} \tag{24}$$

$$f_{3\,t}^{\;explore} = \begin{cases} if\ selected. & f_{3\,t}^{\;explore} = 0 \\ otherwise. & f_{3\,t}^{\;explore} + PF_3 \end{cases} \tag{25}$$

where $Cost_{New.i}^{explore}$ and $Cost_{New.i}^{exploit}$ relates to the *ith* best solution candidate position vector after enhancement in both exploration and exploitation stages; $Cost_{Old.i}^{exploit}$ and $Cost_{Old.i}^{explore}$ refers to the *ith* best solution candidate position vector before enhancement in both exploration and exploitation stages.

3.2. Exploration Phase of Puma Optimizer (PO)

During the exploration phase of the PO algorithm (Fig. 3), the puma's wide-ranging movement across its territory in search of prey is emulated. This phase incorporates two primary strategies: revisiting previously successful hunting sites based on prior experience and exploring new, unvisited areas with high prey potential. These natural behaviors are translated into mathematical mechanisms as follows:

If $rand_1 > 0.5$ $\quad Z_{i.G} = R_{Dim} * (Ub - Lb) + Lb$

Otherwise: (26)

[DOI: 10.22068/ijoce.2026.16.3.671]

$$Z_{i.G} = X_{a.G} + G \cdot (X_{a.G} - X_{b.G}) + G \cdot \Big(\big((X_{a.G} - X_{b.G}) - (X_{c.G} - X_{d.G}) \big) + \big((X_{c.G} - X_{d.G}) - (X_{e.G} - X_{f.G}) \big) \Big)$$

$$G = 2 \times rand_2 - 1 \tag{27}$$

$$X_{new} = \begin{cases} Z_{i.G} . & \text{if } \mathrm{j} = \mathrm{j}_{rand} \quad or \quad rand_3 \leq U \\ X_{a.G}. & otherwise \end{cases} \tag{28}$$

$$NC = 1 - U \tag{29}$$

$$p = \frac{NC}{Npop} \tag{30}$$

$$if \;\; CostX_{new} < CostX_i . \quad U = U + p \tag{31}$$

$$X_{a.G} = X_{new}. \qquad if \; X_{i.new} < X_{a.G} \tag{32}$$

where $R_{Dim}$is a randomly generated number between 0 and 1; Ub and Lb refers to the variables' bounds; $X_{i.G}$ are the randomly selected solution candidates from the entire search space.

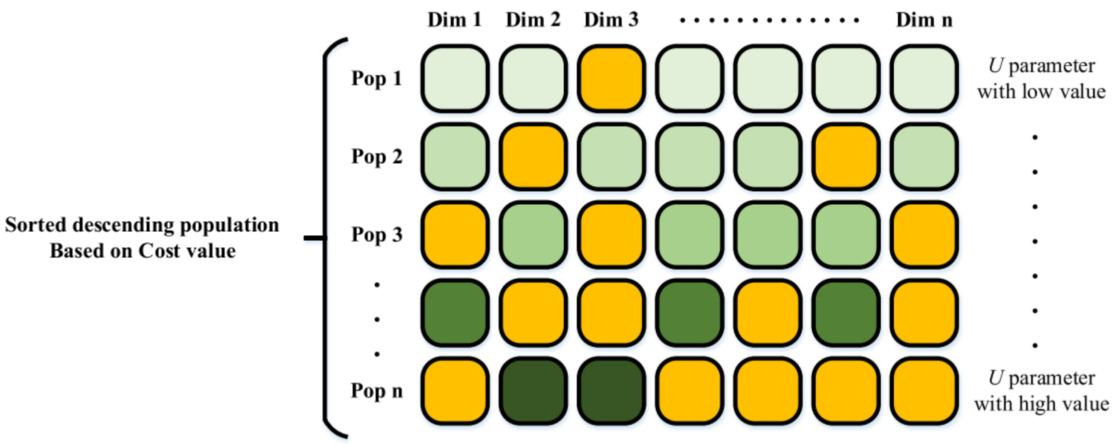

Figure 3: Flowchart of the PO algorithm's exploration phase

3.3. Exploitation Phase of Puma Optimizer (PO)

During the exploitation phase (Fig. 4), the PO algorithm utilizes two specialized operators to intensify the local search around promising solutions. These operators are modeled after the puma's ambush and rapid pursuit (sprinting) hunting behaviors. The mathematical representation of this phase is given by the following equations:

[DOI: 10.22068/ijoce.2026.16.3.671]

[DOI: 10.22068/ijoce.2026.16.3.671]

$$X_{new} = \begin{cases} if\ rand_4 \geq 0{,}5. \quad X_{new} = \dfrac{\left(\dfrac{mean(Sol_{total})}{Npop}\right) \cdot X_1^r - (-1)^\beta \times X_i}{1 + (\alpha \cdot rand_5)} \\ otherwise. \quad if\ \ rand_6 \geq L. \quad X_{new} = Puma_{male} + (2 \cdot rand_7) \cdot exp(randn_1) \cdot X_2^r - X_i \\ otherwise. \quad X_{new} = \ (2 \times rand_8) \times \dfrac{(F_1 \cdot R \cdot X(i)\ +\ F2 \cdot (1-R) \cdot Puma_{male})}{(2 \cdot rand_9 - 1\ +\ randn_2)} - Puma_{male} \end{cases} \tag{33}$$

$$X_2^r = round(1 +\ (Npop - 1) \cdot\ rand_{10}) \tag{34}$$

$$R\ =\ 2 \cdot rand_{11} - 1 \tag{35}$$

$$F_1 = randn_3 \cdot exp\left(2 - Iter \cdot \left(\frac{2}{MaxIter}\right)\right) \tag{36}$$

$$F_2 =\ w \times (v)^2 \cdot cos\big((2 \times rand_{12}) \cdot w\big) \tag{37}$$

$$w = randn_4 \tag{38}$$

$$v = randn_5 \tag{39}$$

Equation (33) describes the two primary strategies employed in the exploitation phase of the PO algorithm, inspired by the puma's hunting behaviors: fast pursuit (running) and ambush tactics.In this formulation, a uniformly distributed random number $rand_5 \in [0,1]$ determines the strategy selection. If $rand_5 > 0.5$, the fast-running strategy is activated, which is mathematically modeled through a division operation to simulate the puma's rapid movement toward prey. Otherwise, the ambush strategy is selected. The ambush strategy itself consists of two distinct operations: short jumps toward other pumas' hunting positions and long jumps toward the best solution (male puma's hunt).

In Equation (32), mean denotes the mean function, Sol_{total} represents the sum of all solutions in the population, and Npop is the population size. X_1^r is a randomly selected solution from the current population, and b is a binary flag (0 or 1) generated randomly. Furthermore, Xi indicates the current solution at iteration i, while α and L are static parameters that must be tuned prior to the optimization process. $Puma_{male}$ represents the best solution (male puma) in the entire population. The terms rand4 to rand9 are uniformly distributed random numbers in [0, 1], exp is the exponential function, and $randn_1$,$randn_2$ are normally distributed random numbers. Finally, X_2^r is a randomly chosen solution selected according to Equation (34).

In the final stage of the PO algorithm, the stopping criterion is checked. Upon satisfaction of this criterion, the best solution found throughout the search process is reported as the optimal result. The pseudocode of the PO algorithm is presented in Fig. 5, and its detailed flowchart is illustrated in Fig. 6.

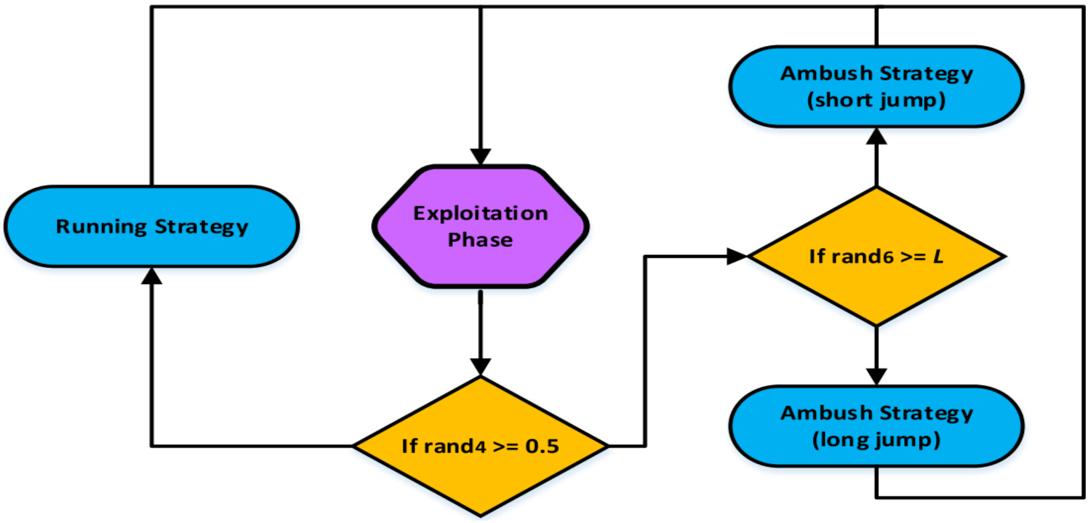

Figure 4: Flowchart of the PO algorithm's exploitation phase

% PO setting
Inputs: The population size N and the maximum number of iterations and parameter settings
Outputs: Puma's location and fitness potential
% initialization
Create a random population using X_i $(i = 1, 2, \ldots, N)$. Calculate Puma's fitness levels.
for iter = 1 : 3
    Apply exploration phase (*Algorithm 1*)
    Apply exploitation phase (*Algorithm 2*)
End
Apply Unexperienced Phase
for iter = 4: *Max iteration*
    Apply experienced Phase
    if $Score_{Explore} > Score_{Exploit}$
        Apply exploration phase (*algorithm 1*)
        if Exploration $NewBestX_i$ Cost < $Puma_{male}$ *Cost*
            $Puma_{male} = NewBestX_i$
        end
    else
        Apply exploitation phase (*algorithm 2*)
        if Exploitation $NewBestX_i$ Cost < $Puma_{male}$ *Cost*
            $Puma_{male} = NewBestX_i$
        end
    end
    Update T, $f1$, $f2$ and $f3$
    Update $Score_{Explore}$ and $Score_{Exploit}$ by Eq. (17)
end

Figure 5: Pseudo code of the PO algorithm

4. UPGRADED PUMA OPTIMIZER (U-PO)

Lévy flights, named after the French mathematician Paul Pierre Lévy, are a class of random walks characterized by step lengths drawn from Lévy stable distributions with heavy-tailed properties. Unlike standard Brownian motion, Lévy flights feature occasional long jumps, enabling significantly faster diffusion and more efficient exploration of large search spaces.

[DOI: 10.22068/ijoce.2026.16.3.671]

This distinctive property makes Lévy flights particularly effective in modeling various natural and complex phenomena, including animal foraging patterns, human mobility, financial market fluctuations, and certain geophysical processes.

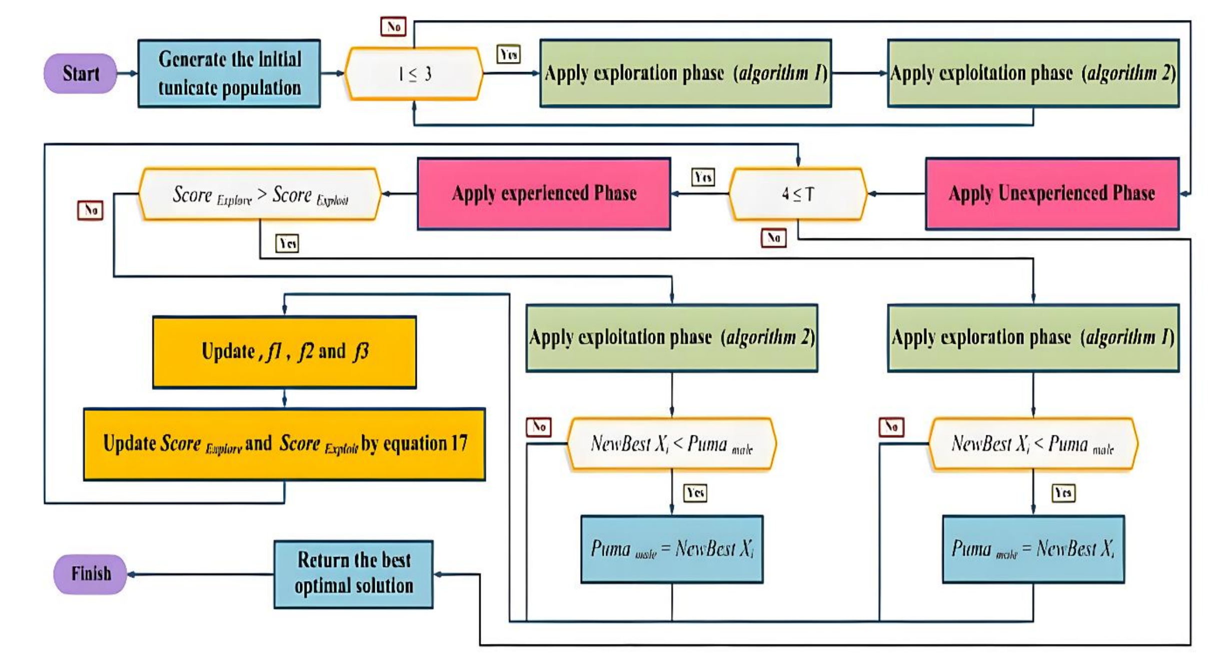

Figure 6: Flowchart of the PO algorithm

From a statistical perspective, Lévy flights exhibit self-affinity and are governed by anomalous diffusion, deviating from the conventional square-root-of-time scaling observed in normal diffusion. These characteristics allow them to better capture irregular, heavy-tailed dynamics in turbulent flows, biological systems with patchy resources, and other environments where extreme events play a significant role.

In the context of metaheuristic optimization, Lévy flights have proven highly effective in enhancing global search capabilities by facilitating escape from local optima through large-scale jumps. Accordingly, the present study investigates the integration of Lévy flights into the Puma Optimizer (PO) to improve its performance. In the proposed Upgraded Puma Optimizer (U-PO), conventional Brownian randomization is replaced with Lévy flight mechanisms. This modification enhances the exploration–exploitation balance, resulting in improved convergence behavior and overall solution quality.The step length in Lévy flights is generated according to the following Lévy distribution:

$$L(s) \sim |s|^{-1-\beta} \tag{40}$$

This distribution can be specified by a Fourier transform:

$$F(k) = exp\left[-\alpha |k|^{\beta}\right]. \qquad 0 < \beta \leq 2 \tag{41}$$

[DOI: 10.22068/ijoce.2026.16.3.671]

The scale parameter α typically complicates the inversion of this integral, as it often lacks a closed-form expression. Notably, when β equals 2, the distribution is Gaussian, and when β is set to 1, it aligns with a Cauchy distribution. In most cases, the inverse of the integral:

$$L(s) = \frac{1}{\pi}\int_0^\infty \cos(ks)\, exp\left[-\alpha|k|^\beta\right] dk \tag{42}$$

$$L(s) \to \frac{\alpha\beta\tau(\beta)\sin(\frac{\pi\beta}{2})}{\pi|s|^{1+\beta}}. \qquad s \to \infty, \tag{43}$$

$$\tau(z) = \int_0^\infty t^{z-1}e^{-t}dt \tag{44}$$

Lévy flights generally outperform conventional Brownian random walks when exploring large and unfamiliar search spaces. This superior efficiency arises primarily from their variable step-length distribution, which can be characterized as follows:

$$\sigma^2(t) \sim t^{3-\beta}. \qquad 1 \le \beta \le 2 \tag{45}$$

To improve the search efficiency of the Puma Optimizer (PO), Lévy flights are integrated into the main loop of the algorithm. This enhancement strengthens the global exploration capability and helps maintain a better balance between exploration and exploitation during the optimization process.

4. STRUCTURAL DESIGN EXAMPLES

For numerical validation and performance evaluation, three steel moment-resisting frames with 1, 10, and 20 stories (Fig. 7) are considered in this study. The single- and 20-story frames have a bay width of 6 m, while the 10-story frame has a bay width of 4 m. All structures feature a uniform story height of 3 m. Steel shear walls are added to these frames to create dual lateral force-resisting systems. Structural analysis and design are performed in accordance with current building codes and standards. The density of steel for both frame members and shear walls is taken as specified in Appendix 6 of the National Building Regulations [26]. A dead load of 500 kg/m² and a live load of 200 kg/m² are applied to the floors and roofs. Seismic loads are determined based on the Iranian Seismic Standard 2800 (4th edition) [27], assuming a high seismic hazard zone with site class III. The design of moment-resisting connections and members follows the requirements of the 10th edition of the National Building Regulations for Steel Structures [28]. The material properties used in the structural design are summarized in Table 1.

[DOI: 10.22068/ijoce.2026.16.3.671]

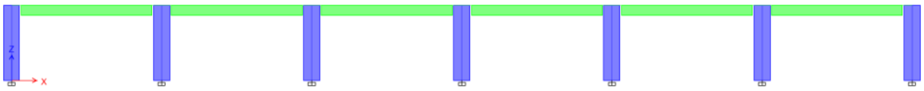

(a)

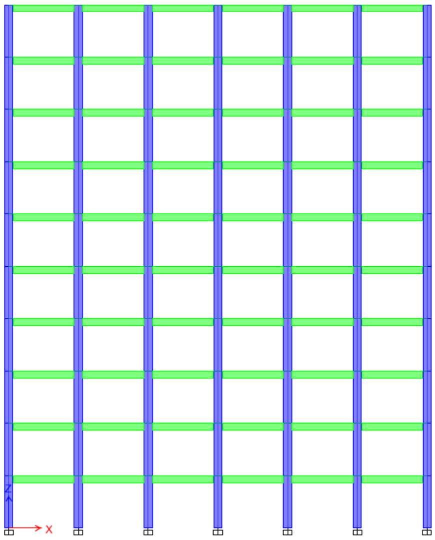

(b)

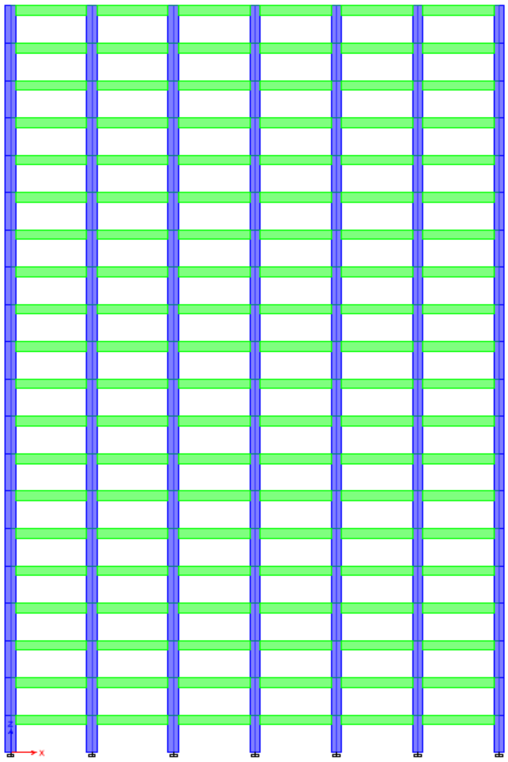

(c)

Figure 7: Schematic view of the 1-story (a), 10-story (b) and 20-story (c) frame structures.

Table 1: Material properties of the steel structural elements.

Property	**Unit weight of steel**	**Yield Strength**	**Ultimate Strength**	**Steel Poisson's Ratio**
Amount	G=7850 kg/m^3	Fy=4000 kg/cm^2	Fu=5000 kg/cm^2	μ=0.3

This section presents the results of the numerical analyses performed using several metaheuristic algorithms, including the Harris Hawks Optimizer (HHO) [23], the Arithmetic Optimization Algorithm (AOA) [24], the Grey Wolf Optimizer (GWO) [25], and the Puma Optimizer (PO) [22]. In addition, the performance of the proposed Upgraded Puma Optimizer (U-PO), which integrates Lévy flights to improve the optimization process, is thoroughly evaluated and compared.

4.1. Case Study 1: One-Story, Six-Bay Dual Steel Frame–Shear Wall System

Figure 8 compares the convergence performance of five metaheuristic algorithms in minimizing the weight of the one-story steel frame structure over 100 iterations. All algorithms begin with relatively high structural weights and exhibit progressive improvement as the optimization proceeds. The Grey Wolf Optimizer (GWO) and the standard Puma

[DOI: 10.22068/ijoce.2026.16.3.671]

Optimizer (PO) demonstrate rapid convergence in the early stages, reaching near-optimal weights before iteration 40. The Harris Hawks Optimizer (HHO) follows a similar trend but with a slightly slower rate. In contrast, the Arithmetic Optimization Algorithm (AOA) shows the slowest convergence, maintaining higher weights until approximately iteration 70.

The proposed Upgraded Puma Optimizer (U-PO) exhibits a more gradual initial reduction; however, it ultimately achieves one of the lowest final weights. The inset plot, which magnifies iterations 80–100, reveals that all algorithms converge to a stable minimum, with U-PO attaining the best final solution. These results indicate that although some algorithms offer faster early convergence, the U-PO provides superior overall performance in terms of solution quality and stability, effectively avoiding premature convergence.

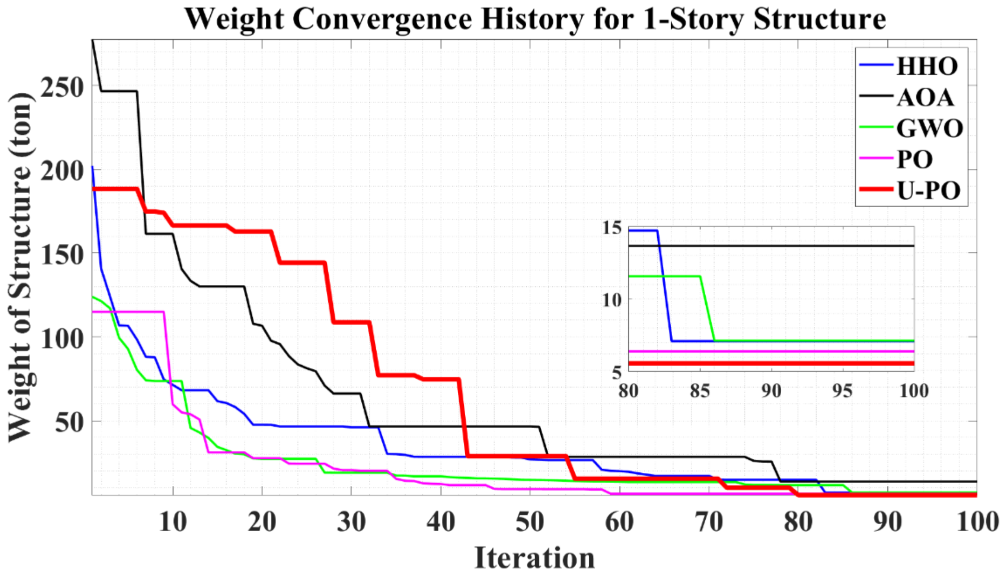

Figure 8: Convergence curves of different metaheuristic algorithms for the one-story steel frame structure

Table 2 summarizes the optimal structural weights obtained for the one-story steel frame using five metaheuristic algorithms, along with the number of spans equipped with steel shear walls. The proposed Upgraded Puma Optimizer (U-PO) achieves the best performance, yielding the minimum weight of 5.56 tons with shear walls placed in only one span. The standard Puma Optimizer (PO) ranks second with a weight of 6.39 tons. The Harris Hawks Optimizer (HHO) and Grey Wolf Optimizer (GWO) produce weights of 7.09 tons and 7.13 tons, respectively, with GWO utilizing two spans with shear walls. In contrast, the Arithmetic Optimization Algorithm (AOA) exhibits the weakest performance, resulting in a significantly higher structural weight of 13.66 tons—approximately 2.5 times greater than that of U-PO. These results demonstrate that the U-PO not only achieves the lightest design but does so with minimal use of shear walls, highlighting its superior efficiency and robustness for structural optimization problems.

Figure 9 presents the optimal distribution of steel shear walls across the bays of the one-story steel moment-resisting frame, as determined by the PO, U-PO, HHO, AOA, and GWO algorithms. Strategic placement of shear walls is essential for improving the lateral stiffness

[DOI: 10.22068/ijoce.2026.16.3.671]

and seismic performance of the structure. The results demonstrate notable differences in the efficiency and configuration of shear wall arrangements produced by the various algorithms. In particular, the proposed Upgraded Puma Optimizer (U-PO) delivers a highly efficient distribution that achieves superior structural performance with minimal reinforcement.

Table 2: Optimal weight of the 1-story structure optimized by different methods.

Metaheuristic Algorithms	No. of Spans with Shear Walls	Weight (ton)
HHO	1	7.09
AOA	1	13.66
GWO	2	7.13
PO	1	6.39
U-PO	1	5.56

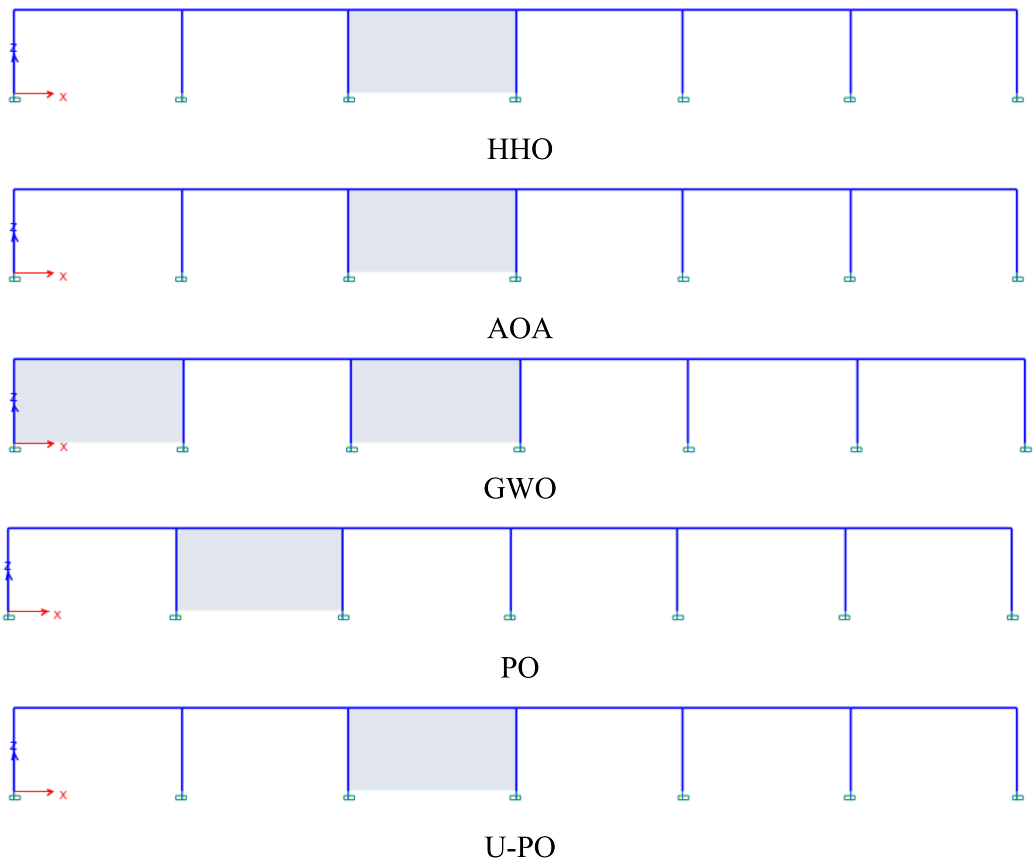

Figure 9: Optimal placement of steel shear walls in the one-story dual steel frame structure obtained by different metaheuristic algorithms.

Figure 10 illustrates the convergence of the penalty function values over 100 iterations for the one-story steel frame structure using five metaheuristic algorithms: HHO, AOA, GWO, PO, and U-PO. At the beginning of the optimization process, all algorithms exhibit relatively high penalty values due to constraint violations. The standard PO shows a sharp spike around iteration 8, indicating temporary instability. Both HHO and AOA experience notable fluctuations in the early and middle stages, with AOA maintaining high penalty values until approximately iteration 50.

In contrast, the Grey Wolf Optimizer (GWO) and the proposed Upgraded Puma Optimizer (U-PO) demonstrate more stable and consistent penalty reduction. The U-PO, in particular, achieves one of the smoothest convergence behaviors, reaching near-zero penalty values around iteration 40 with minimal residual violations. These results indicate that the U-PO not only provides excellent weight minimization but also exhibits superior constraint-handling capability and reliability throughout the optimization process.

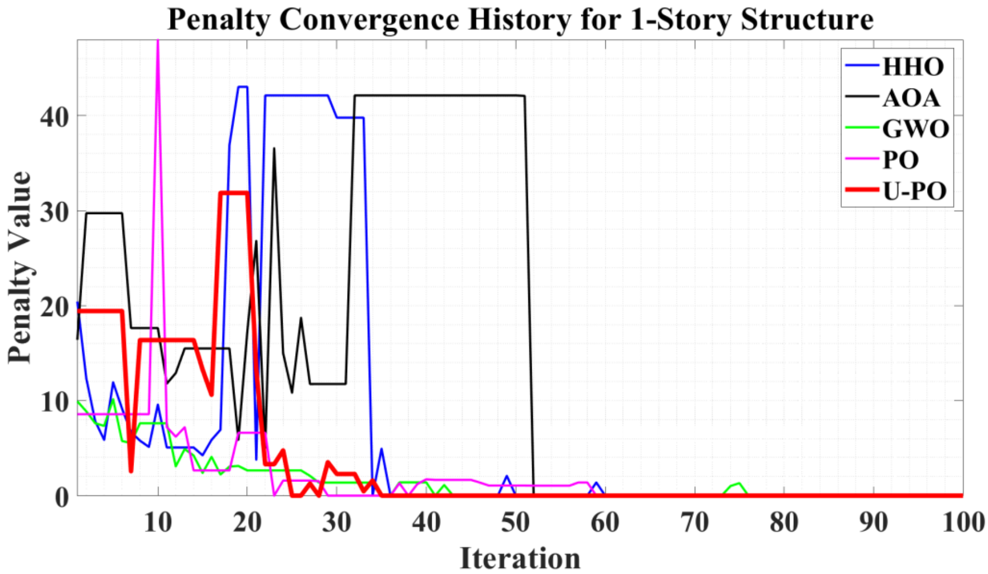

Figure 10: Penalty convergence history of different metaheuristic algorithms for the one-story steel frame structure.

Table 3 presents the optimal steel section profiles selected for columns (C1–C7) and beams (B1–B6) (see Fig. 11) by the five metaheuristic algorithms. Significant differences are observed in the design choices among the algorithms. The proposed Upgraded Puma Optimizer (U-PO) consistently selects lighter sections, such as W4×13, W12×19, and W8×35, which aligns with its superior weight minimization performance observed in the convergence analysis. In contrast, the Arithmetic Optimization Algorithm (AOA) tends to choose considerably heavier sections, including W12×252, W33×263, and W36×232, indicating a more conservative approach focused on satisfying strength and stiffness constraints.

The Harris Hawks Optimizer (HHO) and the standard Puma Optimizer (PO) generally select intermediate section sizes, providing a reasonable balance between weight and structural capacity. The Grey Wolf Optimizer (GWO) exhibits a mixed pattern, with section weights falling between those of AOA and U-PO. While column selections vary notably across algorithms—reflecting different strategies for satisfying combined axial and bending demands—beam sections show more consistent trends, with frequent use of W14 and W18 series.

Overall, the lighter sections chosen by U-PO contribute to its lowest total structural weight, whereas AOA's heavier selections result in higher weights but potentially greater constraint

[DOI: 10.22068/ijoce.2026.16.3.671]

margins. The HHO, GWO, and PO algorithms demonstrate intermediate performance, effectively balancing structural efficiency and design requirements.

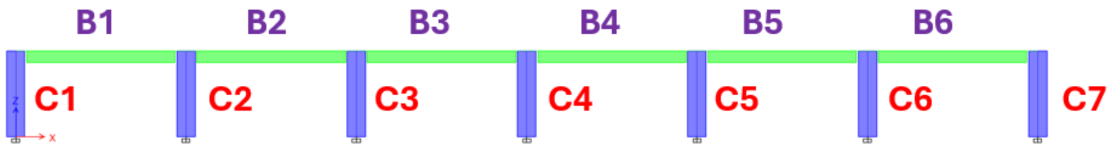

Figure 11: Member numbering of beams (B1–B6) and columns (C1–C7) in the one-story six-bay steel frame structure.

Table 3: Optimal member sections for the one-story steel frame.

	HHO	**AOA**	**GWO**	**PO**	**U-PO**
C1	W21X48	W12X252	W8X15	W33X241	W4X13
C2	W16X45	W6X20	W24X94	W8X31	W18X46
C3	W24X55	W8X21	W10X88	W14X38	W21X55
C4	W10X26	W24X76	W10X26	W4X13	W33X118
C5	W24X84	W24X94	W27X102	W4X13	W14X61
C6	W18X130	W12X35	W8X67	W14X26	W12X19
C7	W40X211	W24X229	W40X362	W12X58	W18X76
B1	W21X44	W33X263	W14X43	W24X176	W14X176
B2	W30X90	W21X111	W14X34	W14X82	W12X22
B3	W10X112	W36X135	W36X135	W21X50	W4X13
B4	W18X35	W21X166	W16X31	W12X50	W36X170
B5	W18X40	W18X258	W21X147	W24X103	W4X13
B6	W30X173	W36X232	W16X31	W21X44	W8X35

4.2. Case Study 2: Ten-Story, Six-Bay Dual Steel Frame–Shear Wall System

Figure 12 presents the weight convergence histories of the five metaheuristic algorithms for the ten-story steel frame structure over 100 iterations. All algorithms start with relatively high structural weights. The Arithmetic Optimization Algorithm (AOA) exhibits the fastest initial convergence, dropping below 400 tons by iteration 15 and continuing to decrease gradually. The Grey Wolf Optimizer (GWO) and the standard Puma Optimizer (PO) show moderate convergence rates, with GWO performing better in the early stages.

The Harris Hawks Optimizer (HHO) demonstrates slower progress initially but achieves competitive results in later iterations. The proposed Upgraded Puma Optimizer (U-PO) starts with a higher initial weight but steadily converges to the lowest final structural weight, as clearly shown in the magnified inset (iterations 80–100). Overall, while all algorithms achieve substantial weight reduction, the U-PO consistently delivers the best optimization performance in terms of final solution quality.

[DOI: 10.22068/ijoce.2026.16.3.671]

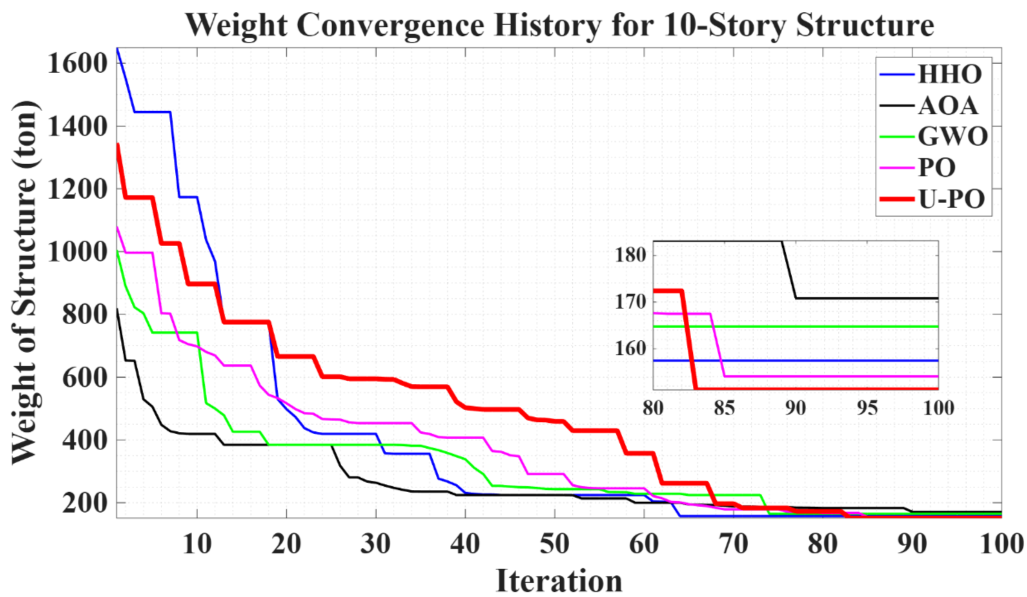

Figure 12: Convergence curves of different metaheuristic algorithms for the ten-story steel frame structure.

Table 4 compares the optimal structural weights and the number of spans equipped with steel shear walls for the ten-story steel frame obtained by different metaheuristic algorithms. The proposed Upgraded Puma Optimizer (U-PO) achieves the best performance, yielding the minimum weight of 151.15 tons with shear walls placed in 27 spans. The standard Puma Optimizer (PO) ranks second with a weight of 154.07 tons, also using 27 shear wall spans.

The Arithmetic Optimization Algorithm (AOA) produces the heaviest design at 170.83 tons with 23 spans. The Grey Wolf Optimizer (GWO) and Harris Hawks Optimizer (HHO) result in intermediate weights of 164.74 tons and 157.44 tons, respectively, both utilizing 20 shear wall spans. These findings demonstrate the superior efficiency of the U-PO in achieving the lightest structural design while maintaining effective seismic performance through optimal shear wall placement.

Table 4: Optimal structural weights and number of shear wall-equipped spans for the ten-story steel frame using various optimization algorithms.

Metaheuristic Algorithms	No. of Spans with Shear Walls	Weight (ton)
HHO	20	157.44
AOA	23	170.83
GWO	20	164.74
PO	27	154.07
U-PO	27	151.15

Figure 13 illustrates the optimal distribution of steel shear walls across the bays of the ten-story steel moment frame for the five metaheuristic algorithms. Shaded areas indicate spans equipped with shear walls. The HHO, GWO, and AOA algorithms tend to concentrate shear walls in fewer locations, primarily in central or side bays, adopting a more localized bracing strategy. In contrast, the PO and especially the proposed U-PO algorithms distribute shear walls more uniformly across multiple spans. The U-PO, in particular, achieves a symmetrical and widespread placement, which contributes to its superior balance between structural weight minimization and lateral stiffness.

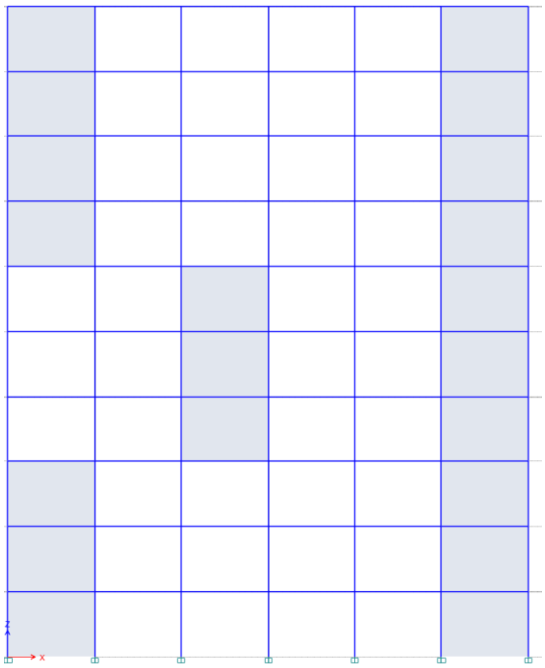

HHO

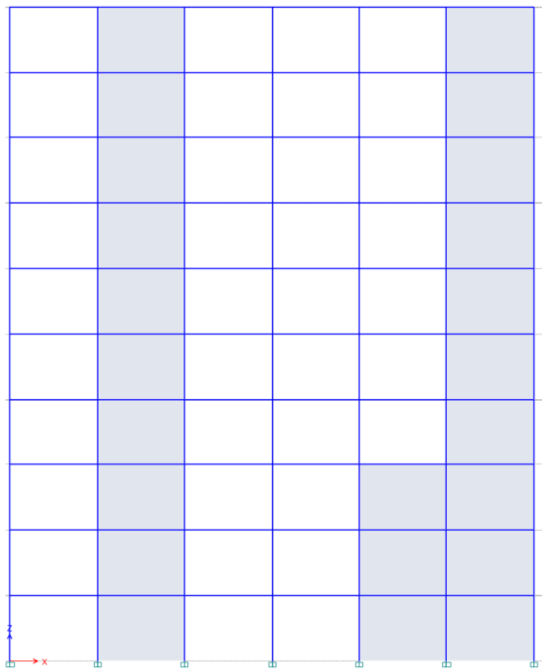

AOA

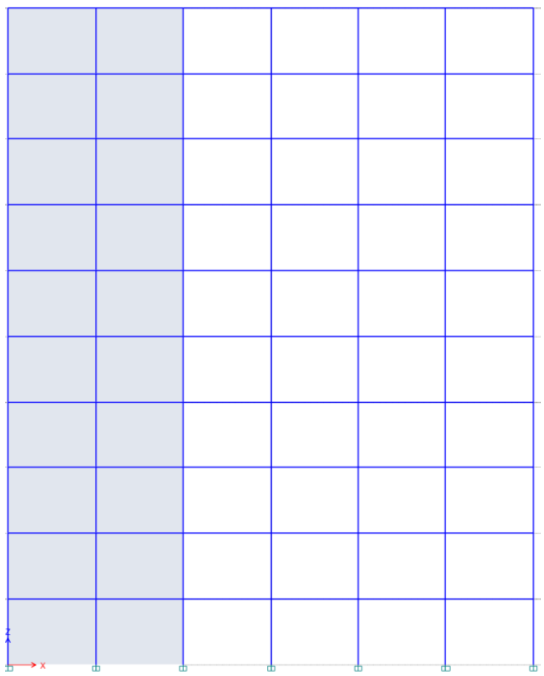

GWO

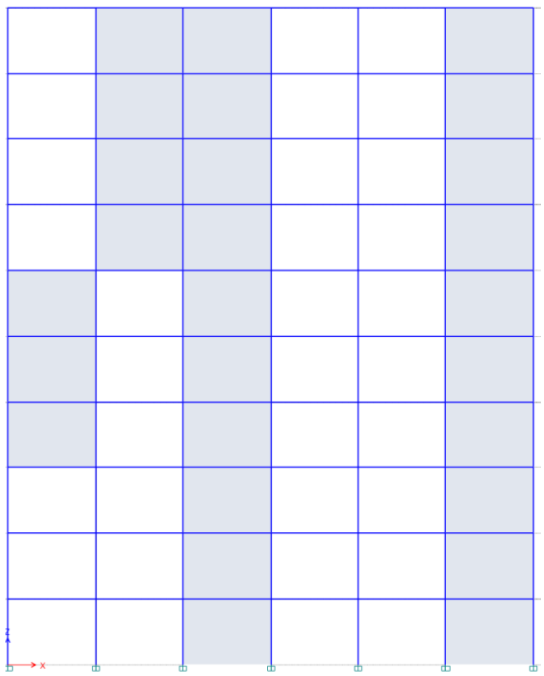

PO

[DOI: 10.22068/ijoce.2026.16.3.671]

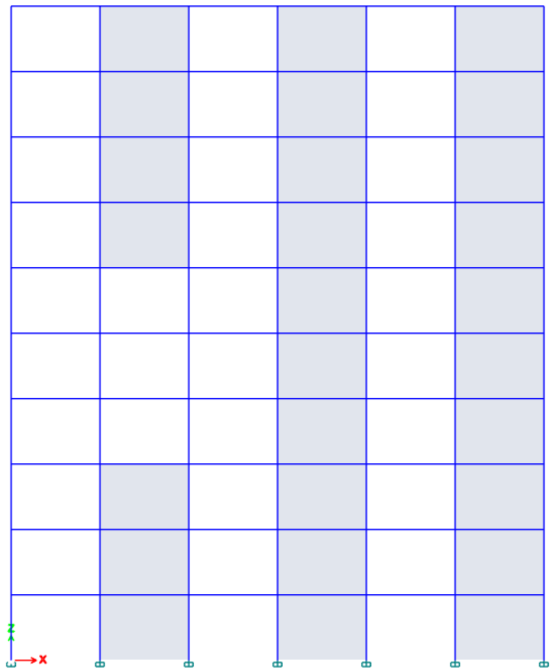

U-PO

Figure 13: Optimal placement of steel shear walls in the ten-story dual steel frame structure obtained by different metaheuristic algorithms.

Figures 14 and 15 present the PMM (P-M-M) interaction ratio convergence histories for a representative column and beam element, respectively, in the ten-story steel frame structure. The performance of the five metaheuristic algorithms (HHO, AOA, GWO, PO, and U-PO) in satisfying strength constraints is compared.

For the selected column (Fig. 14), initial PMM ratios vary among the algorithms, with HHO starting at the highest value (approximately 1.4), while the others begin below 1.0. All algorithms rapidly reduce the interaction ratios. Both AOA and the proposed U-PO maintain the lowest and most stable values (around 0.2–0.3) throughout the optimization process, demonstrating excellent constraint-handling capability.

For the selected beam (Fig. 15), the initial PMM ratios are generally lower across all algorithms. HHO again starts with a slightly higher value but converges rapidly. The U-PO and AOA achieve the most stable and lowest final ratios (approximately 0.1–0.2) with minimal oscillation, whereas PO and GWO exhibit more fluctuations during the early iterations before stabilizing.

Overall, the U-PO consistently exhibits robust and stable performance in satisfying strength constraints for both column and beam members.

[DOI: 10.22068/ijoce.2026.16.3.671]

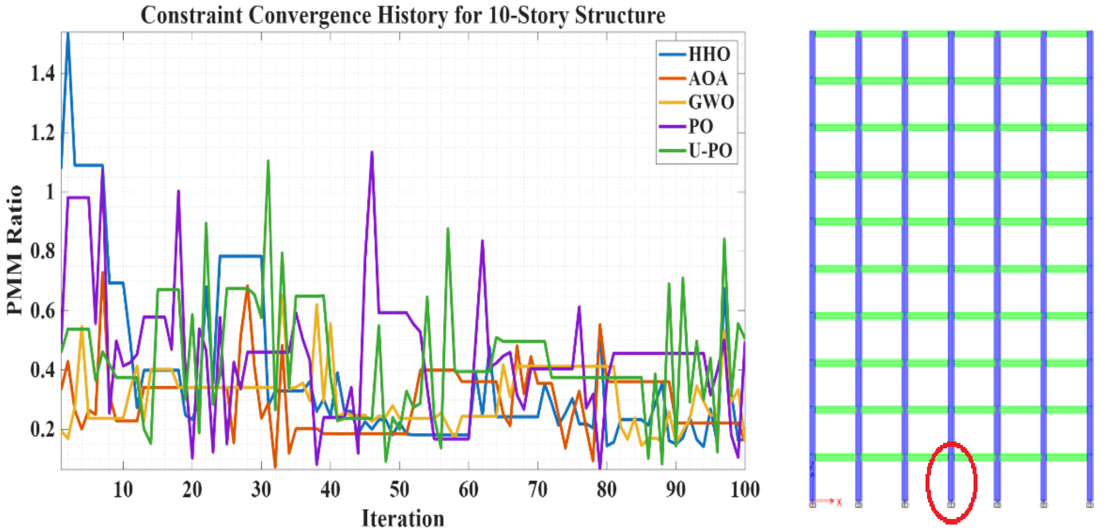

Figure 14: PMM interaction ratio convergence history for a representative column in the ten-story steel frame structure.

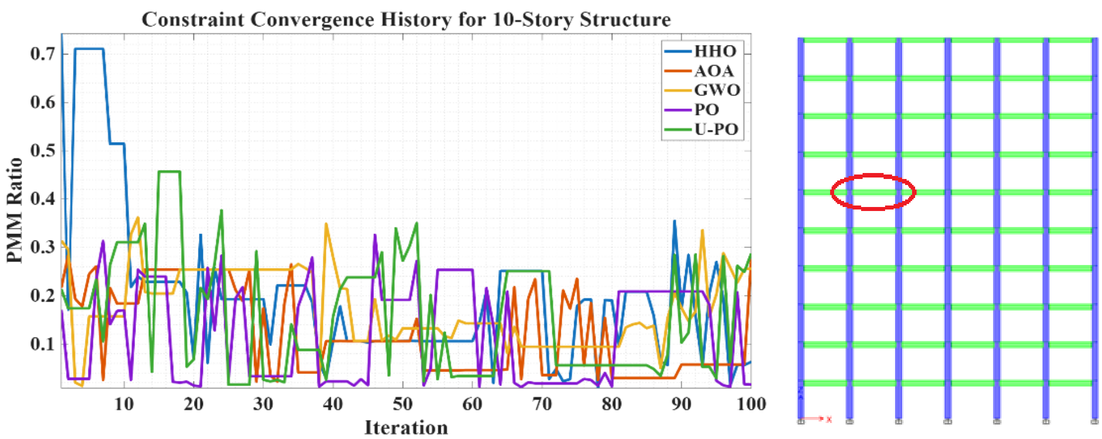

Figure 15: PMM interaction ratio convergence history for a representative beam in the ten-story steel frame structure.

4.3. Case Study 3: Twenty-Story, Six-Bay Dual Steel Frame–Shear Wall System

Figure 16 presents the weight convergence histories of the five metaheuristic algorithms for the twenty-story steel frame structure over 100 iterations. All algorithms start with high initial structural weights. The Arithmetic Optimization Algorithm (AOA) exhibits the fastest convergence, achieving near-optimal values within the first 15 iterations. The proposed Upgraded Puma Optimizer (U-PO) begins with a relatively high weight (approximately 9,000 tons) but demonstrates a rapid reduction in the early stages and consistently converges to the lowest final structural weight, as highlighted in the magnified inset.

The Harris Hawks Optimizer (HHO) shows a slower initial decline but reaches competitive final weights. The standard Puma Optimizer (PO) stabilizes relatively early at around 370 tons, while the Grey Wolf Optimizer (GWO) displays the slowest overall convergence and

[DOI: 10.22068/ijoce.2026.16.3.671]

the highest final weight despite an early sharp drop.

Overall, the U-PO achieves the best optimization performance, delivering the lightest structural design with stable and efficient convergence behavior.

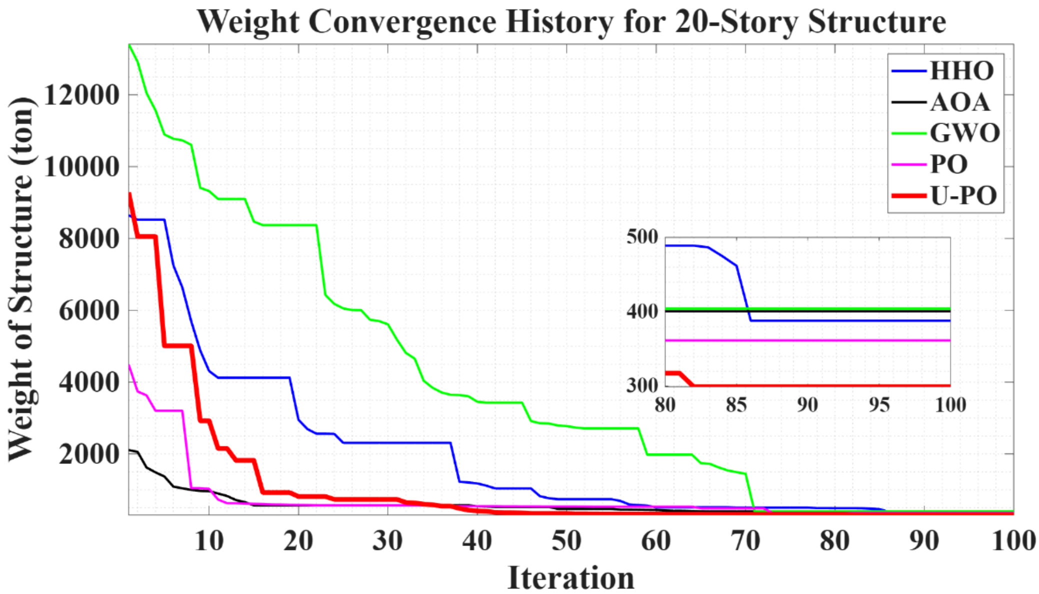

Figure 16: Convergence curves of different metaheuristic algorithms for the twenty-story steel frame structure.

Table 5 compares the optimal structural weights and the number of spans equipped with steel shear walls for the twenty-story steel frame obtained by different metaheuristic algorithms. The proposed Upgraded Puma Optimizer (U-PO) achieves the best performance, yielding the minimum weight of 299.24 tons using 34 shear wall spans. The standard Puma Optimizer (PO) ranks second with a weight of 361.52 tons utilizing 40 spans.

In comparison, the Arithmetic Optimization Algorithm (AOA) and Grey Wolf Optimizer (GWO) result in heavier designs with weights of 400.68 tons (40 spans) and 404.37 tons (57 spans), respectively. The Harris Hawks Optimizer (HHO) produces an intermediate weight of 388.04 tons with 37 shear wall spans. These results demonstrate that the U-PO not only achieves the lightest structural design but does so with a more efficient distribution of shear walls, highlighting its superior material efficiency and overall optimization capability.

Table 5:Optimal structural weights and number of shear wall-equipped spans for the *twenty* -story steel frame using various optimization algorithms.

Metaheuristic Algorithms	No. of Spans with Shear Walls	Weight (ton)
HHO	37	388.04
AOA	40	400.68
GWO	57	404.37
PO	40	361.52
U-PO	34	299.24

[DOI: 10.22068/ijoce.2026.16.3.671]

Figure 17 illustrates the optimal distribution of steel shear walls across the bays of the twenty-story steel moment frame for the five metaheuristic algorithms. Shaded areas represent spans equipped with shear walls. The HHO and AOA algorithms tend to concentrate shear walls along one side of the structure. The GWO distributes them more densely but unevenly across numerous spans, while the PO adopts a relatively balanced yet side-oriented configuration. In contrast, the proposed U-PO achieves a symmetrical and centralized placement, utilizing fewer spans more efficiently. This strategic distribution contributes significantly to the superior performance of U-PO in minimizing the overall structural weight.

Figure 18 presents the inter-story drift ratio convergence history for the 18th story of the twenty-story steel frame structure across the five metaheuristic algorithms. All algorithms begin with drift ratios well below the allowable code limit. The Harris Hawks Optimizer (HHO) shows an initial peak near 0.2, followed by a rapid decrease. The Grey Wolf Optimizer (GWO) consistently maintains the lowest drift ratios (approximately 0.05) throughout the optimization process, demonstrating excellent drift control.

The proposed Upgraded Puma Optimizer (U-PO) and the standard Puma Optimizer (PO) exhibit minor early fluctuations but quickly achieve low and stable drift ratios. The Arithmetic Optimization Algorithm (AOA) displays small oscillations yet remains safely within the allowable limits. In the final iterations, all algorithms converge to stable drift ratios significantly below the code-specified threshold, with GWO and U-PO showing the most consistent low-drift performance.

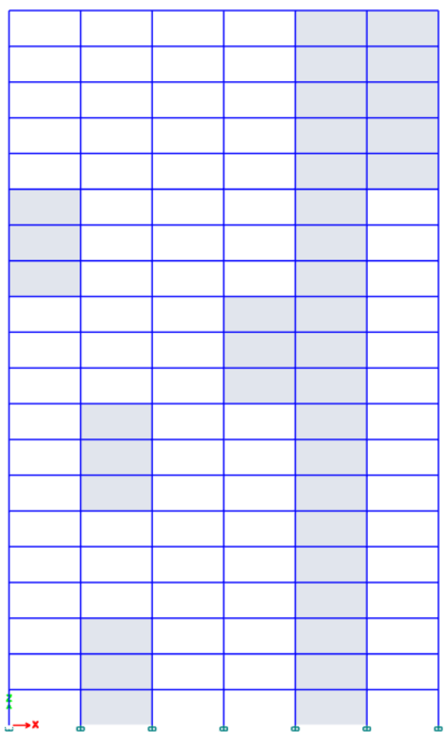

HHO

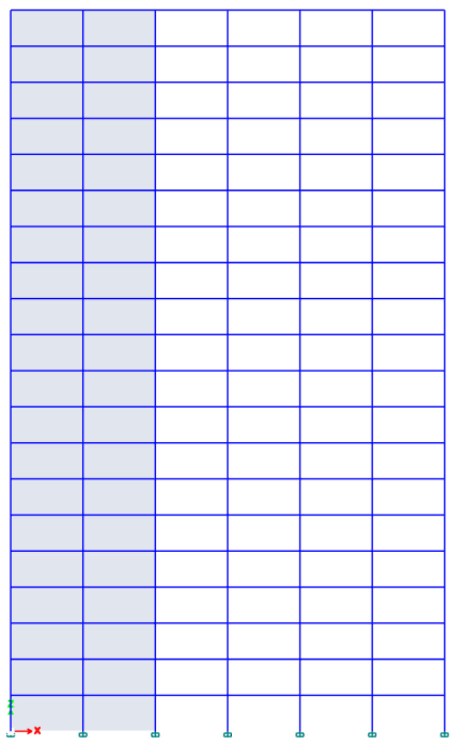

AOA

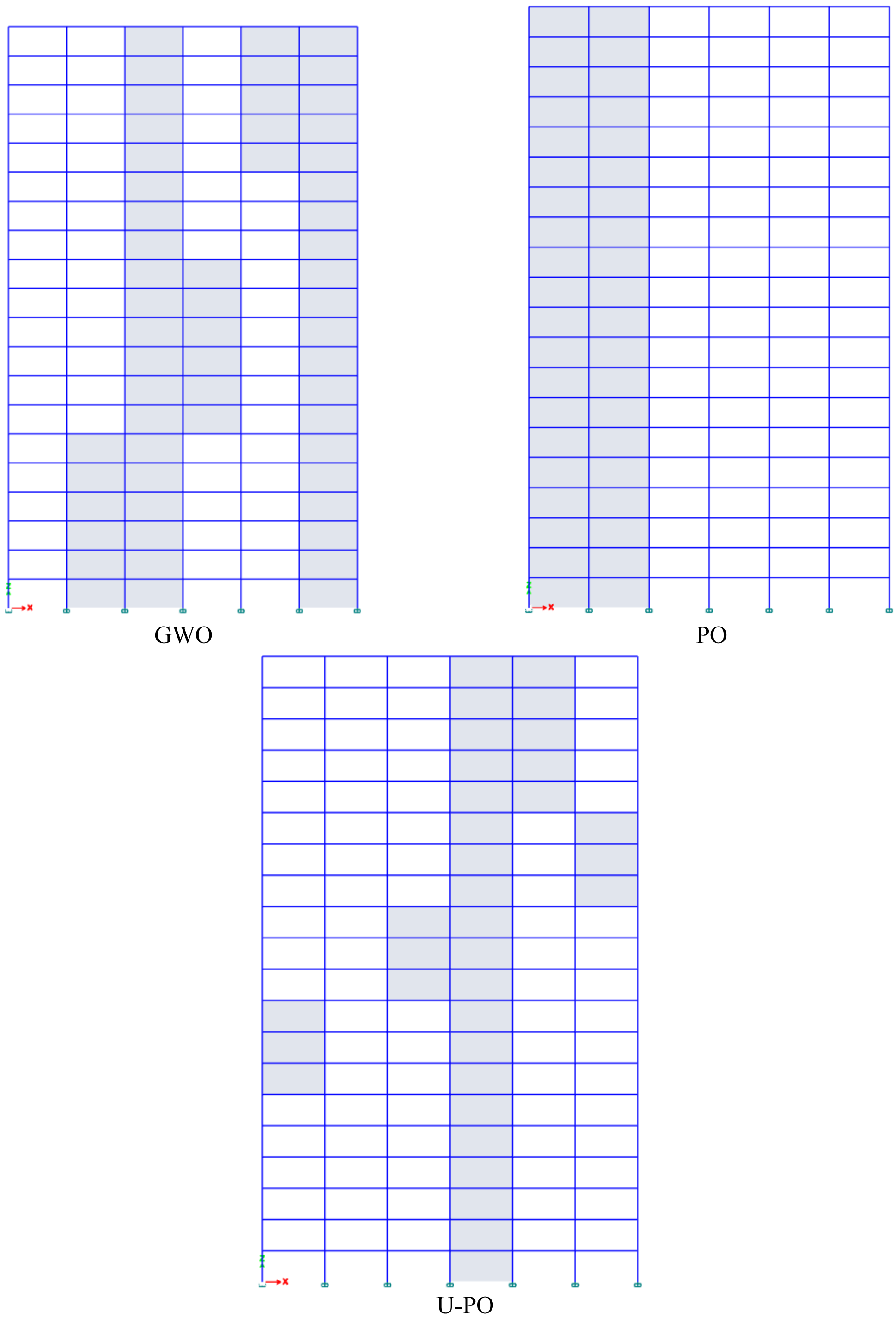

Figure 17: Optimal placement of steel shear walls in the twenty-story dual steel frame structure obtained by different metaheuristic algorithms.

[DOI: 10.22068/ijoce.2026.16.3.671]

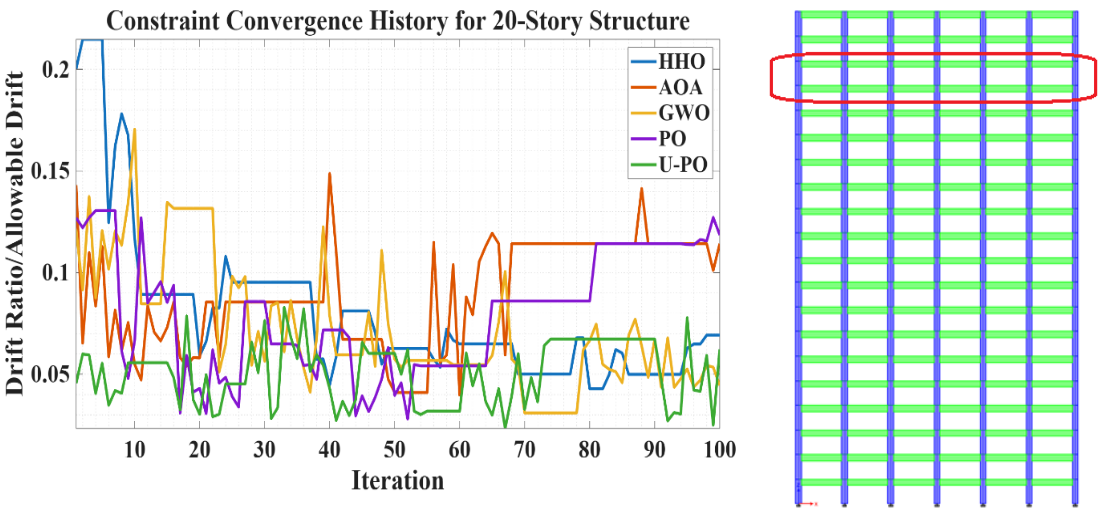

Figure 18: Inter-story drift ratio convergence history at the 18th story of the twenty-story steel frame structure.

4. CONCLUSIONS

This study provides valuable insights into the seismic optimization of dual steel systems consisting of moment-resisting frames and steel shear walls. By employing the standard Puma Optimizer (PO) and the proposed Upgraded Puma Optimizer (U-PO), the research demonstrates significant advancements in structural design efficiency and performance.

A key novelty of this work is the development of the U-PO algorithm, which integrates Lévy flight distribution into the PO framework by replacing conventional Brownian motion randomization. This modification substantially enhances the exploration–exploitation balance, global search capability, and convergence characteristics of the algorithm. The results clearly show that the precise determination of shear wall location, thickness, and mechanical properties is essential for achieving optimal structural performance in terms of strength, safety, and economy. The U-PO consistently achieves substantial reductions in total structural weight through more effective sizing and strategic placement of steel shear walls.

Comparative evaluations against several established metaheuristic algorithms (HHO, AOA, and GWO) confirm the superiority, competitiveness, and robustness of the proposed U-PO. The effectiveness and reliability of the developed approach were successfully validated on three benchmark structures with 1, 10, and 20 stories.

In conclusion, the findings of this study underscore the substantial potential of advanced metaheuristic techniques particularly those enhanced with Lévy flight mechanisms, in modern structural engineering. The proposed U-PO not only advances the theoretical framework of structural optimization but also offers practical and efficient design strategies for developing seismically resilient and cost-effective steel structures.

One-Story Steel Frame:

[DOI: 10.22068/ijoce.2026.16.3.671]

- Thanks to the novel integration of Lévy flights, the proposed U-PO algorithm outperforms all other methods, achieving the lowest structural weight of 5.56 tons. In comparison, the HHO and GWO yield higher weights of 7.09 tons and 7.13 tons, respectively.
- Optimal configurations with shear walls in only one span are obtained by the HHO, AOA, PO, and U-PO algorithms, whereas the GWO requires two spans.
- The U-PO demonstrates superior constraint-handling performance, with one of the smoothest penalty convergence curves, stabilizing at near-zero violations around iteration 40.

Ten-Story Steel Frame:

- Benefiting from the enhanced exploration capability provided by Lévy flights, the U-PO achieves the best performance with a minimum structural weight of 151.15 tons.
- Shear wall distributions vary across algorithms: HHO and GWO utilize 20 spans, AOA uses 23 spans, while both PO and U-PO employ 27 spans.
- The U-PO consistently provides robust and stable satisfaction of strength constraints for both column and beam elements.

Twenty-Story Steel Frame:

- The U-PO attains the lowest structural weight of 299.24 tons, significantly outperforming the competing algorithms. The HHO also delivers competitive results with a weight of 388.04 tons.
- With respect to shear wall placement, HHO and AOA concentrate walls primarily on one side, GWO adopts a dense but uneven distribution, PO shows a relatively balanced yet side-oriented layout, and the U-PO achieves a symmetrical and highly efficient centralized configuration using fewer spans.

Across all three benchmark structures (1-, 10-, and 20-story frames), the proposed U-PO—enabled by the innovative incorporation of Lévy flight mechanisms—demonstrates superior efficiency in minimizing structural weight while effectively satisfying design constraints through optimal shear wall placement and distribution. These results highlight the significant impact of the proposed novelty on both solution quality and computational performance. Future research is recommended to further explore the integration of Lévy flight mechanisms in metaheuristic algorithms and to extend their application to more complex structural systems and diverse design problems.

REFERENCES

1. Banichuk N, Neittaanmäki P. *Structural Optimization with Uncertainties*. Springer; 2009.

[DOI: 10.22068/ijoce.2026.16.3.671]

2. Doltsinis I, Kang Z. Robust design of structures using optimization methods. *Comput Methods Appl Mech Eng*. 2004;**193**:2221–37.
3. Guo X, Cheng G. Recent development in structural design and optimization. *Acta Mech Sin*. 2010;**26**:807–23.
4. Mei LB, Wang Q. Structural optimization in civil engineering: a literature review. *Buildings*. 2021;**11**:66.
5. Sanchez-Caballero S, Selles MA, Pla-Ferrando R, Martinez Sanz, Peydro MA. Recent advances in structural optimization. *Ann Oradea Univ Fasc Manag Technol Eng*. 2012;**1**:118–27.
6. Venkayya V. Structural optimization: a review and some recommendations. *Int J Numer Methods Eng*. 1978;**13**:203–28.
7. Astaneh-Asl A, Qian X, Shi Y. Application of steel shear walls toward more resilient structures. In: *Resilient Structures and Infrastructure*. Springer; 2019.
8. Alinia M, Dastfan M. Behaviour of thin steel plate shear walls regarding frame members. *J Constr Steel Res*. 2006;**62**:730–8.
9. Jahanpour A, Jönsson J, Moharrami H. Seismic behavior of semi-supported steel shear walls. *J Constr Steel Res*. 2012;**74**:118–33.
10. Rahnavard R, Hassanipour A, Mounesi A. Numerical study on important parameters of composite steel–concrete shear walls. *J Constr Steel Res*. 2016;**121**:441–56.
11. Paslar N, Farzampour A, Hatami F. Infill plate interconnection effects on structural behavior of steel plate shear walls. *Thin-Walled Struct*. 2020;**149**:106621.
12. He J, Lin S, Li Y, Dong X, Chen S. Genetic algorithm for optimal placement of steel plate shear walls for steel frames. *Buildings*. 2022.
13. Saedi Daryan A, Salari M, Farhoudi N, Palizi S. Seismic design optimization of steel frames with steel shear wall system using modified dolphin algorithm. *Int J Steel Struct*. 2021.
14. Gholizadeh S, Sojoudizadeh R. Modified sine-cosine algorithm for sizing optimization of truss structures with discrete design variables. *Int J Optim Civ Eng*. 2019;**9**(2):195–212.
15. Kaveh A, Eskandari A. Tuned metaheuristic algorithms for optimal design problems with continuous variables. *Int J Optim Civ Eng*. 2025;**15**(2):259–78.
16. Kaveh A, Eskandari A. Analysis of double-layer barrel vaults using different neural networks: a comparative study. *Int J Optim Civ Eng*. 2021;**11**(1):113–41.
17. Kaveh A, Kamalinejad M, Arzani H. Quantum evolutionary algorithm hybridized with enhanced colliding bodies for optimization. *Structures*. 2020;**28**:1479–501.
18. Kaveh A, Hamedani KB, Kamalinejad M, Joudaki A. Quantum-based jellyfish search optimizer for structural optimization. *Int J Optim Civ Eng*. 2021;**11**(2):329–56.
19. Kaveh A. *Applications of Metaheuristic Optimization Algorithms in Civil Engineering*. Springer; 2017.
20. Kaveh A, Dadras Eslamlou A. *Metaheuristic Optimization Algorithms in Civil Engineering: New Applications*. Springer; 2020.
21. Kaveh A. *Advances in Metaheuristic Algorithms for Optimal Design of Structures*. 3rd ed. Springer; 2021.

22. Abdollahzadeh B, Khodadadi N, Barshandeh S, Trojovský P, Gharehchopogh FS, El-kenawy ES, et al. Puma optimizer (PO): a novel metaheuristic optimization algorithm and its application in machine learning. *Cluster Comput*. 2024.
23. Heidari AA, Mirjalili S, Faris H, Aljarah I, Mafarja M, Chen H. Harris hawks optimization: algorithm and applications. *Future Gener Comput Syst*. 2019;**97**:849–72.
24. Abualigah L, Diabat A, Mirjalili S, Abd Elaziz M, Gandomi AH. The arithmetic optimization algorithm. *Comput Methods Appl Mech Eng*. 2021;**376**:113609.
25. Mirjalili S, Mirjalili SM, Lewis A. Grey wolf optimizer. *Adv Eng Softw*. 2014;**69**:46–61.
26. Iran Building and Housing Research Center. *Minimum Design Loads for Structures*. 2020.
27. Iran Building and Housing Research Center. *Iranian Code of Practice for Seismic Resistant Design of Buildings*, Standard No. 2800, 4th ed. 2020.
28. Iran Building and Housing Research Center. *Seismic Provisions for Structural Steel Buildings*, Part 10. 2020.

[DOI: 10.22068/ijoce.2026.16.3.671]